arXiv:1209.2111v1 [astro-ph.SR] 9 Sep 2012

Phase mixing of standing Alfvén waves with shear flows in solar spicules

H. Ebadi[1] • **M. Hosseinpour**

Abstract

Alfvénic waves are thought to play an important role in coronal heating and solar wind acceleration. Here we investigate the dissipation of such waves due to phase mixing at the presence of shear flow and field in the stratified atmosphere of solar spicules. The initial flow is assumed to be directed along spicule axis and to vary linearly in the x direction and the equilibrium magnetic field is taken 2-dimensional and divergence-free. It is determined that the shear flow and field can fasten the damping of standing Alfvén waves. In spite of propagating Alfvén waves, standing Alfvén waves in Solar spicules dissipate in a few periods. As height increases, the perturbed velocity amplitude does increase in contrast to the behavior of perturbed magnetic field. Moreover, it should be emphasized that the stratification due to gravity, shear flow and field are the facts that should be considered in MHD models in spicules.

Keywords Sun: spicules · Alfvén waves: phase mixing · shear flow · shear field

1 Introduction

Phase mixing has been proposed as a mechanism of efficiently dissipating Alfvén waves in the solar corona by Heyvaerts & Priest (1983). Karami & Ebrahimi (2009) calculated numerically the damping times of standing Alfvén waves in the presence of viscosity and resistivity in coronal loops. They concluded that the exponential damping law obtained by Heyvaerts & Priest (1983) in time is valid for the Lundquist numbers higher than 10^7. De Moortel et al. (1999, 2000) studied the effect of stratification and diverging background magnetic field on phase mixing, and found that the wavelength of an Alfvén wave is shortened as it propagates outwards which enhances the generation of gradients. They concluded that the convection of wave energy into heating the plasma occurs at lower heights than in a uniform model. Moreover, the combined effect of stratification and diverging background magnetic field depends on the geometry of configuration. Smith et al. (2007) showed that the enhanced phase mixing mechanism can dissipate Alfvén waves at heights less than half. Moreover, it can occur in divergent and stratified coronal structures only when the ratio of magnetic and density scale heights is lower than 2.

Kaghashvili (1999) studied the effect of inhomogeneous flow on converting the Alfvén waves into other types of MHD waves that can dissipated efficiently. It is found that in the divergent geometry of magnetic fields, this mechanism becomes essential in the rapidly expanding regions where the velocity shear flow is relatively large. Saleem et al. (2007) studied drift modes driven by shear plasma flow in spicules and concluded that the density inhomogeneity and the shear in the plasma flow should be expected as facts in their atmosphere. These waves propagating on spicules can be efficiently dissipated in the regions with sheared magnetic field in such a way that can heat the solar corona.

Spicules appear as grass-like, thin and elongated structures in images of the solar lower atmosphere (Zaqarashvili & Erdélyi 2009; Sterling 2000). Kukhianidze et al. (2006); Zaqarashvili et al. (2007) by analyzing the height series of $H\alpha$ spectra concluded that transverse oscillations can be caused by propagating kink waves in

---

H. Ebadi

Astrophysics Department, Physics Faculty, University of Tabriz, Tabriz, Iran
e-mail: hosseinebadi@tabrizu.ac.ir

M. Hosseinpour

Plasma Physics Department, Physics Faculty, University of Tabriz, Tabriz, Iran

[1] Research Institute for Astronomy and Astrophysics of Maragha, Maragha 55134-441, Iran.

spicules. De Pontieu et al. (2007); Okamoto & De Pontieu (2011) by making use of *Hinode* observations interpreted that transverse oscillations of spicule axis are signatures of Alfvén waves, and concluded that standing Alfvén waves occurred at the rate of about 20%. More recently Ebadi et al. (2012a) based on *Hinode*/SOT observations concluded that spicule axis oscillations are closed to the standing pattern as they do not see any upward or downward propagation. Ebadi et al. (2012b) performed the phase mixing model of propagating Alfvén waves in spicule conditions and concluded that the damping times are much longer than spicule lifetimes. These results motivated us to study the phase mixing of standing Alfvén waves in a stratified atmosphere in the presence of shear flow and field. To do so, the section 2 gives the basic equations and the theoretical model. In section 3 the numerical results are presented and discussed, and a brief summary is followed in section 4.

2 Theoretical modeling

In the present work we keep the effects of stratification due to gravity in 2D x-z plane in the presence of shear flow and shear field. The phase mixing and dissipation of standing Alfvén waves in a region with non-uniform Alfvén velocity are studied. MHD equations, governing the plasma dynamics are as follows:

$$\frac{\partial \rho}{\partial t} + \nabla \cdot (\rho \mathbf{v}) = 0, \tag{1}$$

$$\rho \frac{\partial \mathbf{v}}{\partial t} + \rho(\mathbf{v}\cdot\nabla)\mathbf{v} = -\nabla p + \rho \mathbf{g} + \frac{1}{\mu}(\nabla \times \mathbf{B}) \times \mathbf{B} + \rho\nu\nabla^2\mathbf{v}, \tag{2}$$

$$\frac{\partial \mathbf{B}}{\partial t} = \nabla \times (\mathbf{v} \times \mathbf{B}) + \eta \nabla^2 \mathbf{B}, \tag{3}$$

$$p = \frac{\rho R T}{\mu}, \tag{4}$$

$$\nabla \cdot \mathbf{B} = 0, \tag{5}$$

where ν and η are constant viscosity and resistivity coefficients, and other quantities have their usual meanings. In particular, typical values for η in the solar chromosphere and corona are $8 \times 10^8 T^{-3/2} \mathrm{m}^2\mathrm{s}^{-1}$ and $10^9 T^{-3/2}$ $\mathrm{m}^2\mathrm{s}^{-1}$, respectively. The value of $\rho\nu$ for a fully ionized H plasma is $2.2 \times 10^{-17} T^{5/2}$ kg m^{-1} s^{-1} (Priest 1982). We assume that the spicules are highly dynamic with speeds that are significant fractions of the Alfvén speed. The perturbations are assumed independent of y, with a polarization in ŷ direction, i.e.:

$$\begin{aligned} \mathbf{v} &= v_0(x)\hat{k} + v_y(x,z,t)\hat{j} \\ \mathbf{B} &= B_{0x}(x,z)\hat{i} + B_{0z}(x,z)\hat{k} + b_y(x,z,t)\hat{j}. \end{aligned} \tag{6}$$

The background flow is assumed to vary linearly in the x-direction as (Poedts et al. 1998):

$$\mathbf{v}_0 = v_0(x)\ \hat{k} = (x-1)v_0\ \hat{k}, \tag{7}$$

and the equilibrium sheared magnetic filed is two-dimensional and divergence-free as (Smith et al. 2007; Murawski & Zaqarashvili 2010):

$$\begin{aligned} B_{0x}(x,z) &= B_0 e^{-k_B z} \sin[k_B(x-1)] \\ B_{0z}(x,z) &= B_0 e^{-k_B z} \cos[k_B(x-1)], \end{aligned} \tag{8}$$

Therefore, the pressure gradient is balanced by the gravity force, which is assumed to be $\mathbf{g}$=-g $\hat{k}$ via this equation:

$$-\nabla p_0 + \rho_0 \mathbf{g} = 0, \tag{9}$$

and the pressure in an equilibrium state is:

$$p_0 = p_0(x) e^{-z/H}. \tag{10}$$

Moreover, the equilibrium density profile is given the form:

$$\rho_0 = \rho_0(x) e^{-z/H}, \tag{11}$$

with

$$H = \frac{RT}{\mu g}, \tag{12}$$

where H is the pressure scale height. Taking into account these assumptions, the linearized dimensionless form of Eqs. 1, 2, and 3 yield:

$$\begin{aligned} \frac{\partial v_y}{\partial t} &= V_A^2(x,z)\left[B_{0x}(x,z)\frac{\partial b_y}{\partial x} + B_{0z}(x,z)\frac{\partial b_y}{\partial z}\right] \\ &\quad - v_0(x)\frac{\partial v_y}{\partial z} + \nu\nabla^2 v_y, \end{aligned} \tag{13}$$

and

$$\frac{\partial b_y}{\partial t} = \left[B_{0x}(x,z)\frac{\partial v_y}{\partial x} + B_{0z}(x,z)\frac{\partial v_y}{\partial z}\right] - v_0(x)\frac{\partial b_y}{\partial z} + \eta\nabla^2 b_y, \qquad (14)$$

where velocities, magnetic field, time and space coordinates are normalized to $V_{A0} \equiv B_0/\sqrt{\mu\rho_0}$ (with ρ_0 as the plasma density at $z = 0$), B_0, τ (Alfvén time), a (spicule radius), respectively. Also the resistivity and viscosity coefficients are normalized to a^2/τ. The first and second terms in the right hand side of Eqs. 13, and 14 representing effects of shear fields and flows, respectively. $V_{\mathrm{A}}(x,z)$ is the Alfvén velocity, which for a phase mixed and stratified atmosphere due to gravity is assumed to be (De Moortel et al. 1999; Karami & Ebrahimi 2009):

$$V_A(x,z) = V_{A0}e^{z/2H}[2 + \tanh[\alpha(x-1)]]. \qquad (15)$$

Here, parameter α controls the size of inhomogeneity across the magnetic field.
The set of Eqs. 13, and 14 should be solved under these initial conditions:

$$\begin{aligned} v_y(x,z,t=0) &= V_{A0}\exp\left[-\frac{1}{2}\left(\frac{x-1}{d}\right)^2\right]\sin(kz)e^{z/4H} \\ b_y(x,z,t=0) &= A\sin(\pi x)\sin(\pi z), \end{aligned} \qquad (16)$$

where d is the width of the initial packet and $A = 10^{-7}$. Figure 1 is the plot of initial wave packet and magnetic field given by Eq. 16 for $d = 0.3a$ (a is the spicule radius). Also, the boundary conditions are taken to be:

$$\begin{aligned} &v_y(x=0,z,t) = v_y(x=2,z,t) = 0 \\ &b_y(x=0,z,t) = b_y(x=2,z,t) = 0, \end{aligned} \qquad (17)$$

and

$$\begin{aligned} &v_y(x,z=0,t) = v_y(x,z=8,t) = 0 \\ &b_y(x,z=0,t) = b_y(x,z=8,t) = 0. \end{aligned} \qquad (18)$$

Boundary conditions in Eq. 18 imply that we are dealing with standing waves.

3 Numerical results and discussion

To solve the coupled Eqs. 13, and 14 numerically, the finite difference and the Fourth-Order Runge-Kutta methods are used to take the space and time derivatives, respectively. We set the number of mesh grid

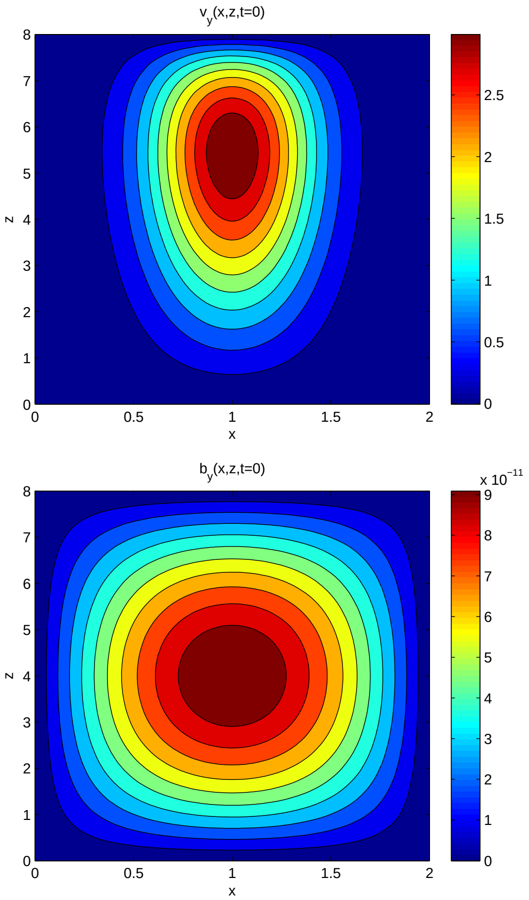

Fig. 1 (Color online) The initial wave packet and magnetic field in $x - z$ space are presented from top to bottom, respectively.

points as 256×256. In addition, the time step is chosen as 0.001, and the system length in the x and z dimensions (simulation box sizes) are set to be (0,2) and (0,8). The parameters in spicule environment are as follows (Murawski & Zaqarashvili 2010; Ebadi et al. 2012a): a (spicule radius)=1000 km, $d = 0.3a = 300km$ (the width of gaussian paket), L=8000 km (Spicule length), $v_0 = 25km/s$, $B_0 = 10G$, $n_e = 10^{11}cm^{-3}$, $T = 8000K$, $g = 272ms^{-2}$, $R = 8300m^2s^{-1}k^{-1}$ (universal gas constant), $V_{A0} = 50km/s$, $k = pi/8$ (dimensionless wavenumber normalized to a), $k_B = pi/16$, $\nu = 10^3m^2s^{-1}$, $\eta = 10^3m^2s^{-1}$, $\mu = 0.6$, $H = 500km$, $\tau = 20$ s, and $\alpha = 2$ (Okamoto & De Pontieu 2011). Figure 2 shows the perturbed velocity variations with respect to time for $x = 1000$ km, $z = 1300$ km; $x = 1000$ km, $z = 4000$ km; and $x = 1000$ km, $z = 6700$ km respectively. We presented the perturbed magnetic field variations, obtained from our numerical analysis, in Figure 3 for $x = 1000$ km, $z = 1300$ km; $x = 1000$ km, $z = 4000$ km; and $x = 1000$ km, $z = 6700$ km respectively. In these plots the perturbed velocity and magnetic field are normalized to V_{A0} and B_0 respectively. In each set of plots it is appeared that both the perturbed velocity and magnetic field are damped at the middle stage of phase mixing.

As height increases, the perturbed velocity amplitude does increase in contrast to the behavior of perturbed magnetic field. This means that with an increase in height, amplitude of velocity oscillations is expanded due to significant decrease in density, which acts as inertia against oscillations. Similar results are observed by time-distance analysis of Solar spicule oscillations (Ebadi et al. 2012a). It is worth to note that the density stratification influence on the magnetic field is negligible, which is in agreement with Solar Optical Telescope observations of Solar spicules (Verth et al. 2011).

Figures 4, 5 show the contour plots of the perturbed velocity and magnetic field with respect to x, z for $t = 10\tau$, $t = 30\tau$, and $t = 100\tau$. They show that in the presence of stratification due to gravity, and shear flow and field the damping takes place in time as an important point of these graphs. In other words, in spite of propagating waves, standing waves are dissipated after a few periods due to phase mixing in the presence of shear flow and field. Once again, increment (decrement) of the perturbed velocity (magnetic) amplitude with height at different times are obvious from these figures. On top of these, latter graphs show stochastic evolution pattern regarding the x-direction. In fact, taking a package of Alfvénic waves with different speeds at different 'x' points results in such non-uniform distribution of oscillations. To be more rigorous, consider

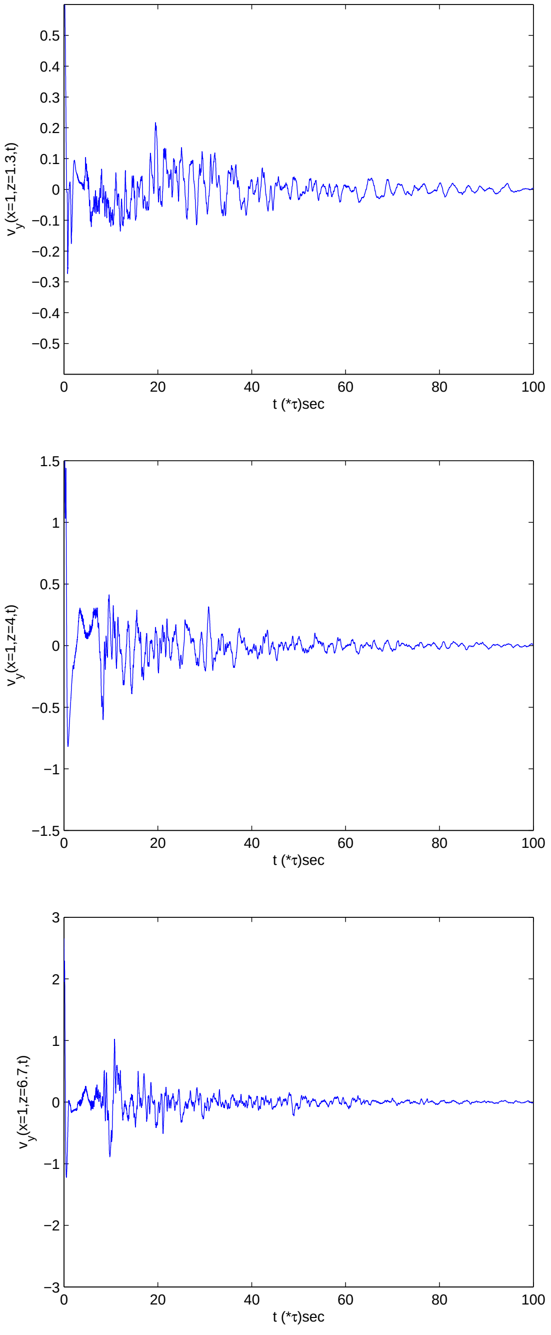

Fig. 2 The perturbed velocity variations with respect to time in $x = 1000$ km, $z = 1300$ km; $x = 1000$ km, $z = 4000$ km; and $x = 1000$ km, $z = 6700$ km respectively from top to bottom are showed.

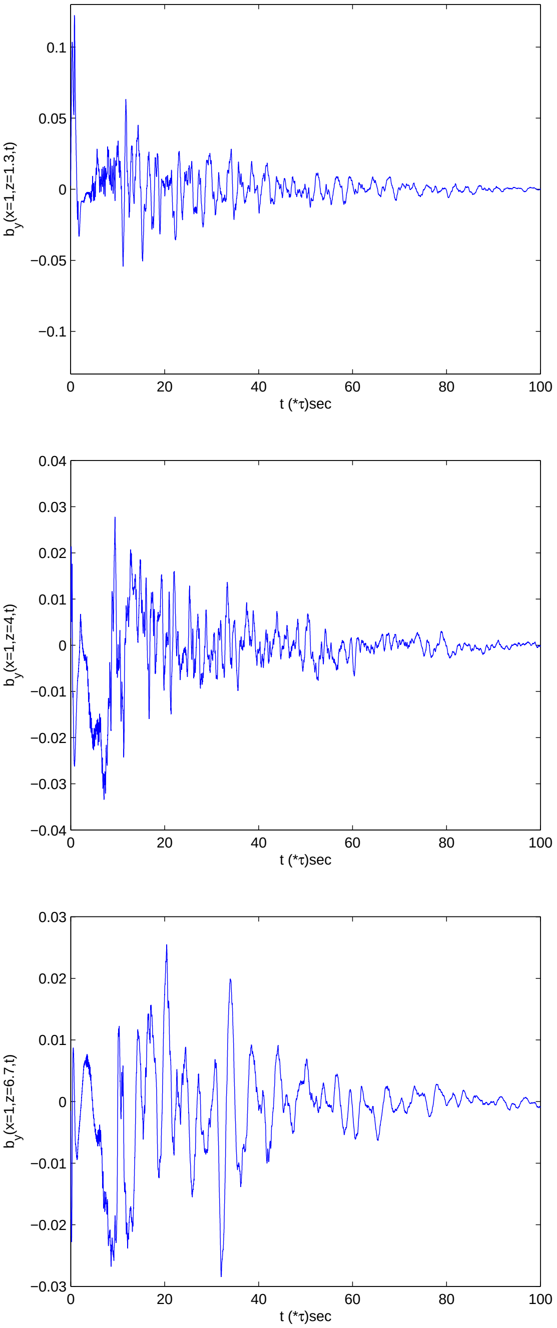

Fig. 3 The same as in Figure 2 but for the perturbed magnetic field.

Eqs. 13, and 14 where the z-derivatives are omitted and main terms are kept only. For instance, one gets:

$$\frac{\partial^2 v_y}{\partial t^2} = V_A^2(x,z)\left[B_{0x}(x,z)\frac{\partial B_{0x}}{\partial x}\frac{\partial v_y}{\partial x} + B_{0x}^2\frac{\partial^2 v_y}{\partial x^2}\right], \tag{19}$$

for the perturbed velocity field. Differential Equation 19, simply, implies that v_y depends to 'x' but unfortunately not in the form of simple function. Additionally, having ignored the z-derivatives, still, v_y varies with 'z' through $V_A(x,z)$ and $B_{0x}(x,z)$ terms. Note that, although, one can discuss about the above point in detail, but, here, we are more interested in studying the effects of phase mixing on time evolution and propagation of Alfvénic waves in the propagation direction rather than looking for variations in the specific perpendicular 'x' direction.

To estimate the damping time it is suitable to calculate the total energy (kinetic energy plus magnetic energy) per unit of length in y direction as:

$$E_{tot}(t) = \frac{16\pi}{B_0^2 aL}\int_0^2 dx \int_0^8 dz[\rho(x,z)v_y^2(x,z) + b_y^2(x,z)]. \tag{20}$$

In Figure 6 the kinetic energy, magnetic energy, and total energy normalized to the initial total energy are presented respectively from top to bottom. It is clear from energy plots that the standing Alfvén waves under spicule conditions can dissipated after a few periods. This is in agreement with the fact that spicules have short lifetimes, and are transient phenomena. The energy flux, stored in oscillating spicule axis, is of the order of coronal energy loss in quiet sun. Therefore, dissipation of standing Alfvén waves can count as a candidate mechanism in transferring and as a result heating the solar corona. Moreover, it should be emphasized that the stratification due to gravity, shear flow and field are the facts that should exist in MHD models in spicules.

4 Conclusion

In our model, we assume that spicules are small scale structures with an initial shear flow and field, and a uniform temperature along them. Density variation along the spicule axis is considerable, and stratification due to gravity is significant. As a result, the medium is dense in its lower heights, but it becomes rare and rare as height increases. The perturbed velocity amplitude does increase in contrast to the behavior of perturbed magnetic field. This means that with

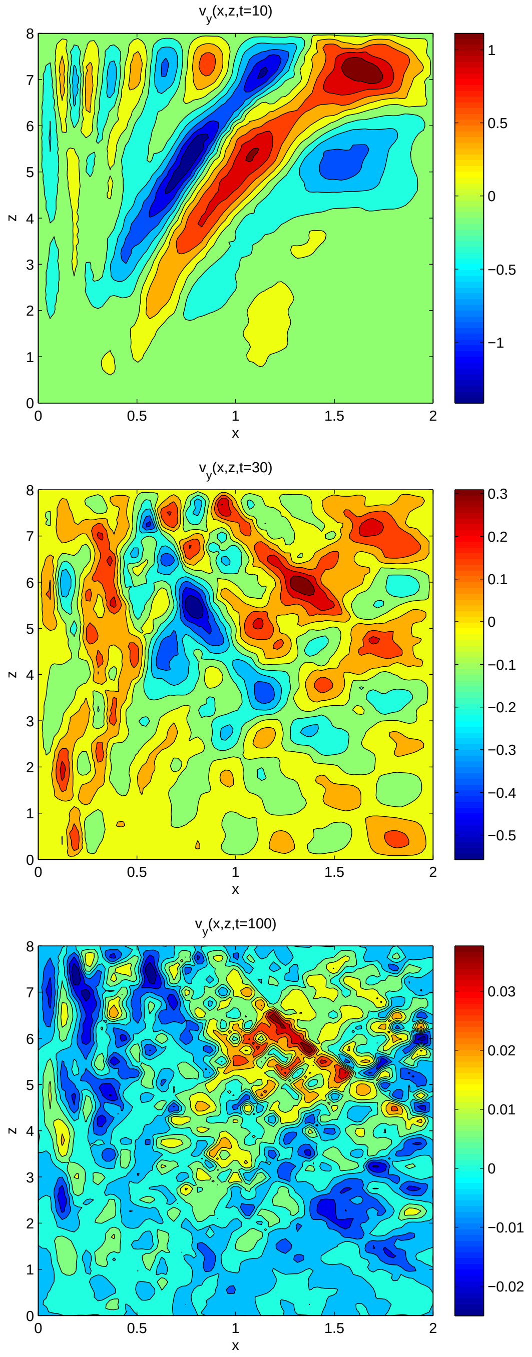

Fig. 4 (Color online) The perturbed velocity in $x-z$ space is presented. The panels from top to bottom correspond to $t = 10\tau$, $t = 30\tau$, and $t = 100\tau$, respectively.

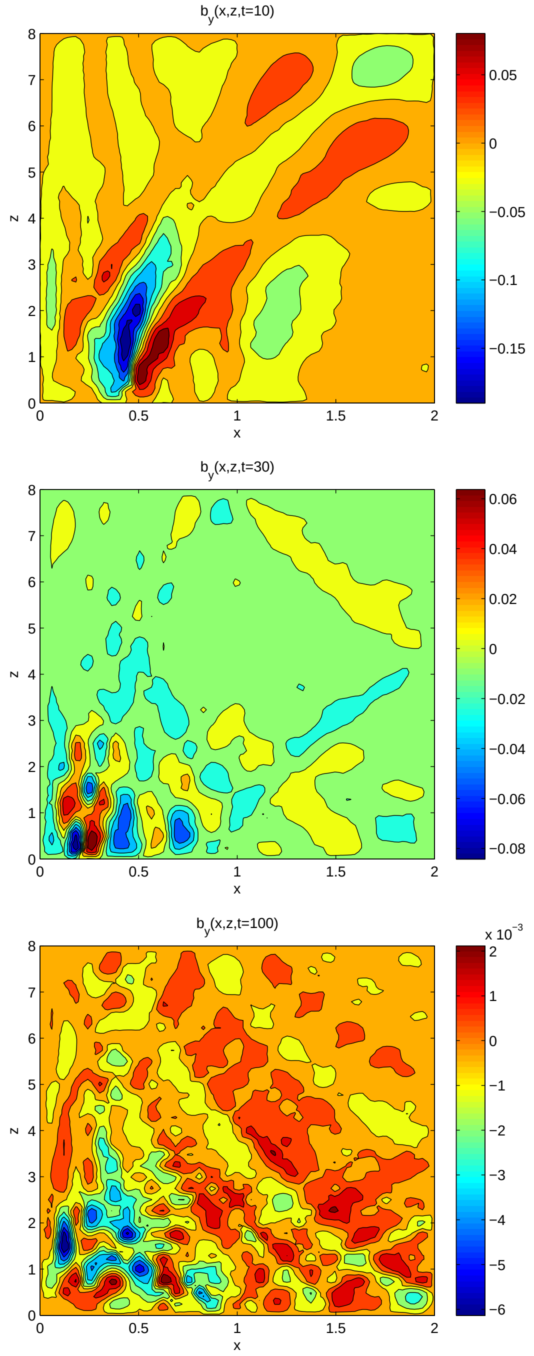

Fig. 5 (Color online) The same as in Figure 4 but for the perturbed magnetic field.

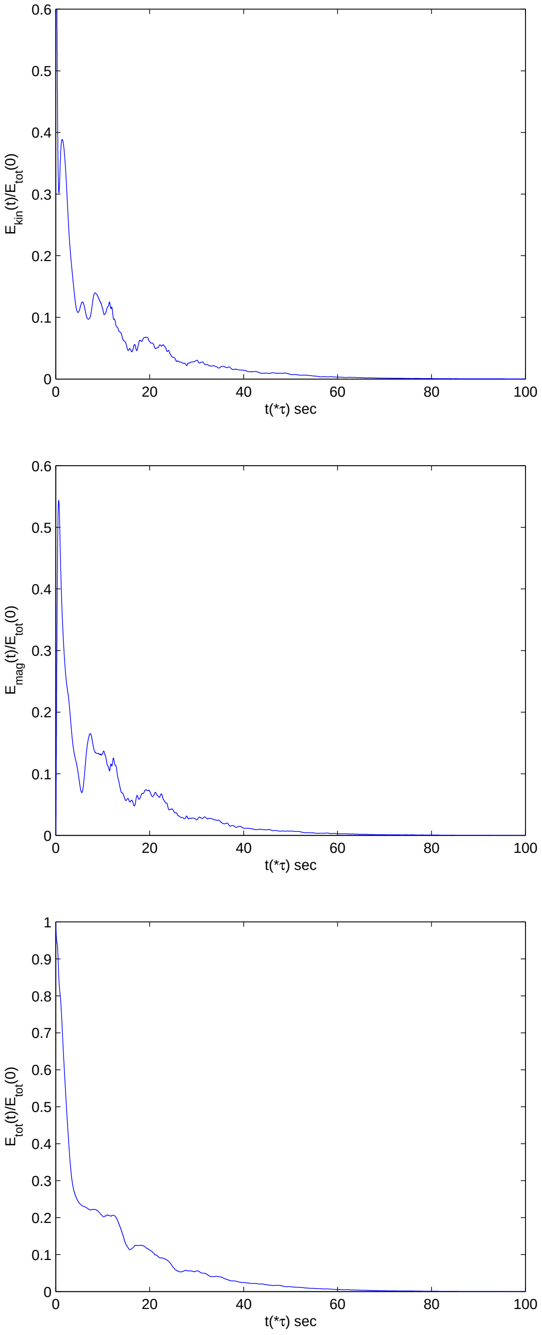

Fig. 6 Time variations of normalized kinetic energy, magnetic energy, and total energy for $d = 0.3a$ are presented from top to bottom respectively.

an increase in height, amplitude of velocity oscillations is expanded due to stratification. It is worth to note that the density stratification influence on the magnetic field is negligible. The divergent configuration of initial magnetic field with sheared plasma flow can fasten the phase mixing and dissipation of standing Alfvén waves in Spicules. This is in agreement with the fact that spicules have short lifetimes, and are disappeared after a few periods.

Acknowledgements This work has been supported financially by the Research Institute for Astronomy and Astrophysics of Maragha (RIAAM), Maragha, Iran.

References

De Moortel, I., Hood, A.W., Arber, T.D.: Astron. Astrophys. **346**, 641 (1999)

De Moortel, I., Hood, A.W., Ireland, J., Arber, T.D.: Astron. Astrophys. **354**, 334 (2000)

De Pontieu, B., McIntosh, S.W., Carlsson, M., et al.: Science **318**, 1574 (2007)

Ebadi, H., Zaqarashvili, T.V., Zhelyazkov, I.: Astrophys. Space Sci. **337**, 33 (2012)

Ebadi, H., Hosseinpour, M., Altafi-Mehrabani, H.: Astrophys. Space Sci. **340**, 9 (2012)

Heyvaerts, J., Priest, E.R.: Astron. Astrophys. **117**, 220 (1983)

Kaghashvili, E.K.: Astrophys. J. **512**, 969 (1999)

Karami, K., Ebrahimi, Z.: Proc. Astron. Soc. Aust. **26**, 448 (2009)

Kukhianidze, V., Zaqarashvili, T. V., Khutsishvili, E.: Astron. Astrophys. **449**, 35 (2006)

Murawski, K., Zaqarashvili, T.V.: Astron. Astrophys. **519**, A8 (2010)

Okamoto, T.J., De Pontieu, B.: Astrophys. J. **736**, 24 (2011)

Priest, E.R. 1982, Solar Magnetohydrodynamices, Dordrecht: Reidel

Poedts, S., Rogava, A.D., Mahajan, S.M. 1998, Astrophys. J. **505**, 369 (1998)

Saleem, H., Vranjes, J., Poedts, S. 2007, Astron. Astrophys. **471**, 289 (2007)

Smith, P. D., Tsiklauri, D., Ruderman, M. S. 2007, Astron. Astrophys. **475**, 1111 (2007)

Sterling, A.C. 2000, Sol. Phys. **196**, 79 (2000)

Verth, G., Goossens, M., He, J.-S.: Astrophys. J. Lett. **733**, 15 (2011)

Zaqarashvili, T.V., Erdélyi, R.: Space Sci. Rev. **149**, 335 (2009)

Zaqarashvili, T. V., Khutsishvili, E., Kukhianidze, V., Ramishvili, G.: Astron. Astrophys. **474**, 627 (2007)

This manuscript was prepared with the AAS LaTeX macros v5.2.